Fire Properties of Polystyrene−Clay Nanocomposites

Jin Zhu,[†] Alexander B. Morgan,[§,||] Frank J. Lamelas,[‡,⊥] and Charles A. Wilkie*[,†]

Departments of Chemistry and Physics, Marquette University, P.O. Box 1881, Milwaukee, Wisconsin 53201, and Fire Science Division, Building and Fire Research Laboratory, National Institute of Standards and Technology, Gaithersburg, Maryland 20899[#]

Received December 31, 2000. Revised Manuscript Received February 13, 2001

Polystyrene−clay nanocomposites have been prepared using a bulk polymerization technique. Three new "onium" salts have been used to prepare the nanocomposites, two are functionalized ammonium salts while the third is a phosphonium salt. By TGA/FTIR, both ammonium and phosphonium treatments have been shown to degrade by a Hofmann elimination mechanism at elevated temperatures. TGA/FTIR showed that the phosphonium treatment is the most thermally stable treatment when compared to the two ammonium salts. The nanocomposites were characterized by X-ray diffraction, transmission electron microscopy, strength and elongation at break, as a measure of the mechanical properties, thermogravimetric analysis, and cone calorimetry. The onset temperature of the degradation is increased by about 50 °C and the peak heat release rate is reduced by 27−58%, depending upon the amount of clay that is present. The mass loss rates are also significantly reduced in the presence of the clay.

Introduction

Nanocomposites, composed of clay and polymer, have been studied extensively for some time and it has been shown that most of the properties are enhanced in the presence of a small amount of clay.[1] For instance, a polyamide-6 clay nanocomposite, containing 5% clay, shows an increase of 40% in tensile strength, 68% in tensile modulus, 60% in flexural strength, and 126% in flexural modulus, while the heat distortion temperature increases from 65 to 152 °C and the impact strength is lowered by only 10%.[2]

The nanocomposite is typically comprised of an organically modified clay and some polymer. The clay that is most commonly used is montmorillonite, MMT, which is an aluminosilicate mineral with sodium counterions present between the clay layers. This space between the clay layers is referred to as the clay gallery. To make this compatible with organic polymers, the sodium counterions are usually ion-exchanged with an organic ammonium or phosphonium salt to convert this material into a hydrophobic ammonium- or phosphonium-treated clay. The nanocomposites may be prepared either by a blending process, either melt blending or solution blending, or by a polymerization process in the presence of the organically modified clay.

In this paper we describe the preparation of three new organically modified clays and the preparation of nanocomposites of these clays by bulk polymerization. The type of nanocomposite that was produced was elucidated using X-ray diffraction and transmission electron microscopy. The properties of these polymer−clay nanocomposites were characterized by thermogravimetric analysis, cone calorimetry, and strength and elongation at break, as a measure of mechanical properties.

Experimental Section

Materials. The majority of chemicals used in this study, including styrene, triphenylphosphine, 2,2′-azobis(isobutyronitrile) (AIBN), and inhibitor removal columns were acquired from Aldrich Chemical Co. TCI America was the supplier for *n*-hexadecyl chloride. Pristine sodium montmorillonite was supplied by Southern Clay Products, Inc.

Instrumentation. Infrared spectroscopy, FTIR, was performed on a Mattson Galaxy infrared spectrometer at 4-cm^{-1} resolution. Thermogravimetric analysis (TGA) was performed on an Omnitherm 1000 unit under a flowing nitrogen atmosphere at a scan rate of 10 °C/min from 20 to 600 °C. Thermogravimetric analysis coupled with Fourier transform infrared spectroscopy, TGA/FTIR, was carried out using a Cahn model 131 balance interfaced to a Mattson Galaxy infrared spectrometer under an inert atmosphere at a flow rate of 40 cm/min. All TGA results are the average of a minimum of three determinations; temperatures are repeatable to ±3 °C while the error bars on the fraction of nonvolatile material is ±3%. Cone calorimetry was performed using a Stanton-Redcroft/PL Thermal Sciences instrument according to ASTM E 1354-92 at an incident flux of 35 kW/m^2 using a cone-shaped heater. Exhaust flow was set at 24 L/s and the spark was continuous until the sample ignited. Cone samples were prepared by compression molding the sample (20−50 g) into square plaques, using a heated press. All cone samples were

* To whom correspondence should be addressed.
[†] Department of Chemistry, Marquette University.
[‡] Department of Physics, Marquette University.
[§] National Institute of Standards and Technology.
[||] Current address: The Dow Chemical Company, Nanomaterials Group, Midland, MI 48674.
[⊥] Current address: Department of Physics, Boise State University, Boise, ID 83725-1570.

[#] It is the policy of the National Institute of Standards and Technology to use the International System of Units (metric units) in its technical communications. However, in this document other units are used to conform to the publisher's style. Further, the contributions of the author from the National Institute of Standards and Technology (NIST), an agency of the U.S. government, by statute is not subject to copyright in the United States.

(1) Alexandre, M.; Dubois, P. *Mater. Sci. Eng.* **2000**, *R28*, 1−63.
(2) Kojima, Y.; Usuki, A.; Kawasumi, M.; Okada, A.; Fukushima, Y.; Kurauchi, T.; Kamigaito, O. *J. Mater. Res.* **1993**, *8*, 1185−1189.

10.1021/cm000984r CCC: $20.00
Published on Web 04/28/2001

run in duplicate and typical results from cone calorimetry are reproducible to within about ±10%.[3] X-ray scattering measurements were performed using a Rigaku powder diffractometer, with a Cu tube source ($\alpha = 1.54$ Å) operated at 1 kW. Bright field transmission electron microscopy (TEM) images of polystyrene/layered silicate (clay) nanocomposites were obtained at 120 kV, at low-dose conditions, with a Phillips 400T electron microscope. The samples were ultramicrotomed with a diamond knife on a Leica Ultracut UCT microtome at room temperature to give 70-nm-thick sections. The sections were transferred from water to carbon-coated Cu grids of 200 mesh. The contrast between the layered silicates and the polymer phase was sufficient for imaging, so no heavy metal staining of sections prior to imaging was required. Elemental analysis was done by Midwest Microlab. Mechanical testing was performed using an Instron tester.

Synthesis of *n*-Hexadecyl Triphenylphosphonium Chloride. In a round-bottom flask were placed 10.44 g (0.0402 mol) of *n*-hexadecyl chloride and 10.50 g (0.0401 mol) of triphenylphosphine and the mixture was maintained at 80 °C for 10 h. The final viscous product was washed with petroleum ether three times and dried overnight at 50 °C. ^{1}H NMR (D_2O): δ 7.72−7.38 (m, 15 H), 3.25 (br, 2 H), 1.41 (br, 2 H), 1.20−1.04 (m, 26 H), 0.73 (t, $J = 6.0$ Hz, 3 H). ^{13}C NMR (D_2O): δ 134.92 (d, $J = 8.8$ Hz), 130.95 (d, $J = 13.5$ Hz), 118.50 (d, $J = 91.5$ Hz), 32.55, 30.91, 30.70, 30.06, 29.84, 29.70, 23.25, 23.00, 14.53. ^{31}P NMR (D_2O): δ 23.89.

Synthesis of 4-(Chloromethyl)benzyl Alcohol.[4] A 3.86-g (20-mmol) sample of 4-(chloromethyl)benzoyl chloride was dissolved in 150 mL of anhydrous THF in a 250-mL three-necked flask equipped with stirrer, addition funnel, and nitrogen inlet. A 3.09-g (80-mmol) portion of $NaBH_4$ was added, followed by 300 mL of EtOH/THF (1/1, v/v). The solution was stirred for 3 h at room temperature and then concentrated to about 50 mL using a rotary evaporator. About 400 mL of a 3% w/w solution of $NaHCO_3$ in distilled water was added and the solution was then extracted with 400 mL of ether. The ether solution was washed with 500 mL of water and 500 mL of NaCl water solution and then dried with $MgSO_4$ overnight. After recrystallization from ether/cyclohexane (1/4, v/v), 2.5 g of 4-(chloromethyl)benzyl alcohol (yield = 80%) was obtained. MS: 156/158 (3/1) for mother ion M^+. ^{1}H NMR($CDCl_3$): δ 7.37−7.28 (m, 4 H), 4.70 (s, 2 H), 4.59 (s, 2 H), 2.88 (s, 1 H). ^{13}C NMR ($CHCl_3$): δ 141.94, 137.40, 129.56, 127.92, 65.23, 46.73. mp 58−60 °C.

Synthesis of *N,N,N*-Trimethyl-(4-vinylbenzyl)ammonium Chloride (VB-1).[5,6] A 9.12-g (0.071-mol) sample of 4-chloromethylstyrene was added to 16.52 g of 25% (w/w) trimethylamine (0.070 mol) in methanol at 0 °C in the presence of 0.5 wt % hydroquinone and the solution was stirred for 8 h at 0 °C; then, the solution was permitted to warm to room temperature and the stirring was continued overnight. The methanol was evaporated and 50 mL of acetone was added. A white precipitate (8.2 g) of *N,N,N*-trimethyl-(4-vinylbenzyl)-ammonium chloride (yield = 84%) was filtered and washed several times with acetone and then dried overnight at room temperature. The NMR spectra agreed with those which have been previously reported.[5,6]

Syntheses of *N,N*-Dimethyl-*n*-hexadecyl-(4-vinylbenzyl)ammonium Chloride (VB-16) and *N,N*-Dimethyl-*n*-hexadecyl-(4-hydroxymethylbenzyl) Ammonium Chloride (OH-16). The procedure is similar to that of Muzny et al., who synthesized hexadecyltrimethylammonium chloride.[7] A 10.80-g (0.0387-mol) portion of *N,N*-dimethyl-*n*-hexadecylamine was combined with 4.56 g of 4-vinylbenzyl chloride (0.0356 mol) in 40 mL of ethyl acetate and the solution was stirred at 40 °C overnight. The white precipitate of *N,N*-dimethyl-*n*-hexadecyl-(4-vinylbenzyl)ammonium chloride was recovered by filtration, and after recrystallization from ethyl acetate, 12.5 g was obtained (yield = 86%). ^{1}H NMR (D_2O): δ 7.38−7.18 (m, 4 H), 6.52 (dd, $J = 10.5$, 17.4 Hz, 1 H), 5.70 (d, $J = 17.4$ Hz,1 H), 5.12 (d, $J = 10.2$ Hz, 1 H), 4.40 (s, 2 H), 2.90 (s, 6 H), 2.73 (br, 2 H), 1.63 (br, 2 H), 1.38−0.96 (m, 26 H), 0.88 (t, $J = 6.0$ Hz, 3 H). ^{13}C NMR (D_2O): δ 139.22, 136.83, 133.85, 128.48, 127.18, 115.49, 66.49, 61.87, 51.63, 32.81, 30.70, 30.50, 29.31, 26.40, 23.32, 22.40, 14.64. Replacement of 4-vinylbenzyl chloride with 4-hydroxymethylbenzyl chloride produces OH-16-treated montmorillonite. ^{1}H NMR (D_2O): δ 7.43−7.28 (m, 4 H), 4.38 (s, 2 H), 3.05 (br, 2 H), 2.93 (s, 6 H), 1.73 (br, 2 H), 1.30−1.05 (m, 26 H), 0.80 (t, $J = 6.0$ Hz, 3 H) (note: CH_2OH is about 4.60, which is overlapped by solvent). ^{13}C NMR (D_2O): δ 141.41, 133.64, 128.47, 126.86, 67.10, 63.47, 63.05, 51.70, 32.72, 30.60, 30.47, 30.36, 30.27, 29.78, 26.80, 23.39, 23.05, 14.60.

Preparation of Ammonium-Modified Clays. A suspension of 25 g of prewashed sodium montmorillonite, Na−MMT, in 1 L of distilled water was stirred overnight in an Erlenmeyer flask. To the stirred, cooled (0−5 °C) suspension, an aqueous solution of 30 mmol of the organic ammonium salt synthesized above in 100 mL of water was added dropwise. After the solution was stirred for 3 h at 0−5 °C, the white precipitate was filtered, washed with water until no chloride ion could be detected by an aqueous $AgNO_3$ solution, and then dried in a vacuum oven overnight at room temperature. The clay was placed in petroleum ether and stirred for 1 h, followed by filtration and washing with additional petroleum ether. This procedure results in the formation of a powdery clay that can be easily dispersed in monomer. The clay was finally dried in vacuo overnight at room temperature.

Preparation of Phosphonium-Modified Clays. A procedure similar to that for the ammonium clays was followed except that the precipitated clay was dried in vacuo overnight at room temperature and then at 70 °C for 24 h.

Preparation of PS−Clay Nanocomposites. The nanocomposites were prepared following the procedure that has been previously described.[8] In a 200-mL beaker were placed 3 g of organically modified clay, 1 g of *N,N′*-azobis(isobutyronitrile) (AIBN) as a radical initiator, and 100 g of monomeric styrene. This mixture was treated as follows: stirring at room temperature under flowing N_2 gas until it became a homogeneous suspension; heating to 80 °C for a few minutes to prepolymerize and then cooling to room temperature; polymerizing at 60 °C for 24 h and at 80 °C for another 24 h under a N_2 atmosphere. Unreacted monomer was then removed under vacuum (0.1 mmHg) for 6 h at 100 °C to obtain the nanocomposite.

Measurement of Molecular Weight. The nanocomposites were extracted using toluene at room temperature and repeatedly filtered to ensure the removal of the clay, and then the molecular weights were determined by viscosity measurements. A bulk polymerization of polystyrene was carried out at the same time that the nanocomposites were prepared, using the same procedure except for the absence of the clay. The viscosity average molecular weight of the extracted polymers from all preparations and from the polystyrene prepared as a control was 100 000 ± 20 000.

Results and Discussion

The organic modifications that have been used for this work were carefully chosen to illustrate particular points. The structures of these salts are shown in Figure 1. VB-16 contains a styrene functionality on the ammonium salt and it is expected that some of the polymerization will involve the salt along with some

(3) Gilman, J. W.; Kashiwagi, T.; Nyden, M.; Brown, J. E. T.; Jackson, C. L.; Lomakin, S.; Gianellis, E. P.; Manias, E. In *Chemistry and Technology of Polymer Additives*; Al-Maliaka, S., Golovoy, A., Wilkie, C. A., Eds.; Blackwell Scientific: London, 1998; pp 249−265.
(4) Pierce, M. E.; Harris, G. D.; Islam, Q.; Radesca, L. A.; Storace, L.; Waltermire, R. E.; Wat, E.; Jadhav, P. K.; Emmett, G. C. *J. Org. Chem.* **1996**, *61*, 444−450.
(5) Akelah, A.; Moet, A. *J. Mater. Sci.* **1996**, *31*, 31589−31596.
(6) Akelah, A.; Moet, A. *Mater. Lett.* **1993**, *18*, 97−102.
(7) Muzny, C. D.; Butler, B. D.; Hanley, H. J. M.; Tsvetkov, F.; Peiffer, D. G. *Mater. Lett.* **1996**, *28*, 379−384.
(8) Zhu, J.; Wilkie, C. A. *Polym. Intern.* **2000**, *48*, 1158−1163.

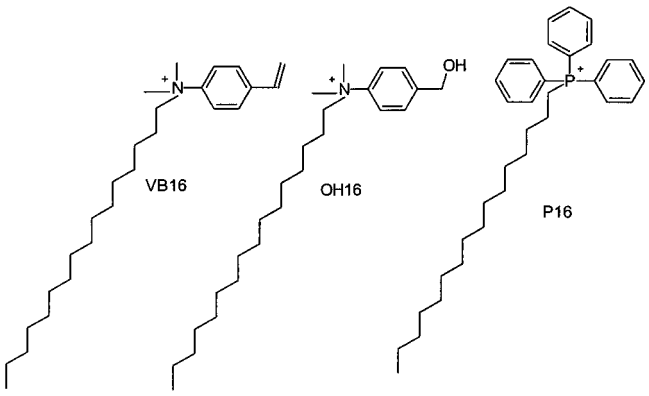

Figure 1. Structures of the salts used to prepare the organically modified clays.

Scheme 1. Degradation of an "Onium" Salt To Give an Olefin, an Amine, and a Proton as the Counterion for the Clay

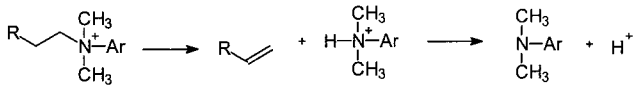

simple radical polymerization involving only the added styrene. Thus, the polymerization can occur in the clay gallery, "tethering" or linking the polymer to the clay surface by a covalent bond to the ammonium cation. A related material, vinylbenzyldodecyldimethylammonium-modified clay has recently been reported.[9] OH-16 contains a benzyl alcohol functionality; in previous work we have shown that such an alcohol functionality can undergo Friedel−Crafts chemistry and thereby affect cross-linking of the polymer chain.[10] Thus, upon heating, one may expect to incorporate some fraction of the polymer onto the salt-modified clay. That is, the same type of tethering that may occur with VB-16 can also occur with OH-16 but the latter will only undergo this type of reaction at temperatures above about 250 or 300 °C. A related salt, trimethyl(4-vinylbenzyl)ammonium (VB-1), was also synthesized and the preparation of the polystyrene nanocomposite was attempted. According to the literature, a nanocomposite may be prepared by solution polymerization.[5,6] The bulk polymerization process that is used in this study is ineffective because this material does not disperse well in monomeric styrene. Finally, the phosphonium salt was chosen for investigation of the differences between organo ammonium and phosphonium salt treatments of clay fillers in nanocomposites.

TGA/FTIR Characterization of Organically Modified Clays. Xie[11] has published on the degradation of organically modified clays and has suggested that a Hofmann elimination reaction occurs, producing an olefin and an amine and, of necessity, leaving a proton occupying the cationic position on the clay. The essentials of this reaction are shown as Scheme 1. It is well-known that "onium" salts will participate in such a reaction[12] and the thermal degradation of an ammonium counterion in a clay has been reported to lose ammonia and give a proton counterion.[13]

Table 1. TGA/FTIR Results for the Thermal Degradation of the Organo-Treated Clays

temp range, °C	mass loss, %	IR peaks observed, cm^{-1}	products
		VB-16 Clay	
185−235	1	2933, 2860, 2769, 1460	hexadecene
235−340	10	2933, 2860, 2769, 1720, 1460	hexadecene, hexadecanal, or hexadecanone
340−400	7	2970, 2933, 2860, 1460	hexadecene,
400−600	8	3017, 2970, 2933, 2860, 1460	$Me_2NCH_2-C_6H_4-CH=CH_2$
		OH-16 Clay	
210−250	2	2951, 2933, 2886, 1460	hexadecene
250−340	6	2951, 2933, 2886, 2769, 1749, 1510	hexadecene, hexadecanal, or hexadecanone
340−370	8	2951, 2933, 2866, 1510	hexadecene
170−560	16	3017, 2968, 2933, 2886, 1510	hexadecene, $Me_2NCH_2PhCH_2OH$
		P-16 Clay	
240−290	2	2931, 2840	hexadecene
290−340	9	2931, 2840, 1722	hexadecene, hexadecanal, or hexadecanone
340−490	19	3065, 2931, 2840	hexadecene, PPh_3
490−600	5	3065, 1427, 1196, 1117	PPh_3

An aldehyde arising from the thermal degradation of a dodecyl-substituted ammonium salt but not from a octadecyl salt has been identified in previous work.[11] TGA/FTIR studies on these clays confirm the presence of a carbonyl compound, along with aliphatic and aromatic species, and the results are shown in Table 1. For instance, for the VB-16 clay, elemental analysis indicates that the clay consists of 24% organic cation and 76% clay. The TGA shows the loss of 26% mass, which roughly corresponds to the loss of all of the organic cation. The cation consists of 58% hexadecyl and therefore hexadecyl loss should correspond to a total of 15% mass loss and the amine to 11%. The actual values observed are 18% hexadecyl and 8% amine. The intensity of the double-bond stretch is always quite low so it is not surprising that it is not seen in this study. The identification of the evolution of hexadecene is based on the observation of the C−H stretching frequency due to an aliphatic material and the agreement with previous work. All compounds were identified by matching the observed frequencies with those in standard reference books.[14] The formation of a carbonyl species is surprising and difficult to explain; the most likely explanation is some catalytic activity of the clay causing the oxidation to a carbonyl species.

A similar analysis may be carried out on the other two clays. These results serve to confirm the previous observation of a Hofmann elimination as the degradation pathway of the clay. The TGA curves for all three clays are shown in Figure 2. One can see the cor-

(9) Fu, X.; Qutubuddin, S. *Mater. Lett.* **2000**, *42*, 12−15.
(10) Wang, Z.; Jiang, D. D.; McKinney, M. A.; Wilkie, C. A. *Polym. Degrad. Stab.* **1999**, *64*, 387−395. Zhu, J.; McKinney, M. A.; Wilkie, C. A.; *Polym Degrad. Stab.* **1999**, *66*, 213−220. Wang, Z.; Jiang, D. D.; Wilkie, C. A.; Gilman, J. W.; *Polym. Degrad. Stab.* **1999**, *66*, 373−378.
(11) Xie, W.; Gao Z.; Pan, W.-P.; Vaia, R.; Hunter, D.; Singh, A. *Polym. Mater. Sci. Eng.* **2000**, *83*, 284.
(12) Jones, M., Jr. *Organic Chemistry*, 2nd ed.; W. W. Norton & Co. Inc.: New York, 2000; p 258.
(13) Wright, A. C.; Granquist, W. T.; Kennedy, J. V. *J. Catal.* **1972**, *25*, 65−80.
(14) Conley, R. T. *Infrared Spectroscopy*, 2nd ed.; Allyn and Bacon: Boston, MA, 1972.

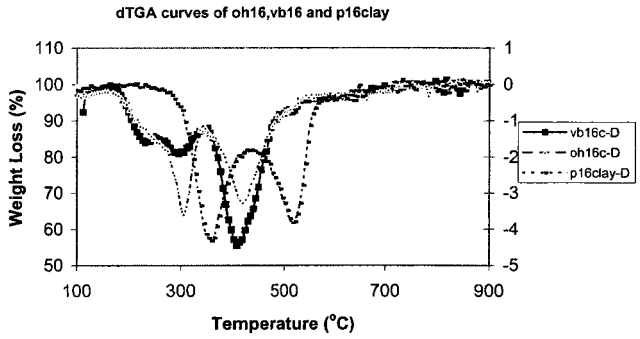

Figure 2. TGA curves for VB-16 and OH-16 clays under an inert atmosphere.

Table 2. XRD Data for Clays and Nanocomposites from Those Clays

clay	d_{001}, clay, nm	d_{001}, nanocomposite, nm
Na−MMT	.96	
VB-16	2.87	
OH-16	1.96	3.53
P-16	3.72	4.06

respondence between the tabular data and the TGA curves and the enhanced thermal stability of the phosphonium clay. This implies that a phosphonium clay may be an advantage in instances where a higher thermal stability for the treated clay is needed. The thermal instability of the ammonium salts has been a problem in the processing of thermoplastics above 200 °C. These phosphonium materials, or other salts in which the Hofmann elimination is rendered difficult, may prove useful when such high-temperature processing conditions are required.

The formation of a nanocomposite involves the insertion of the polymer between the layers of the clay. There are two terms that are used to describe the general classes of nanocomposites, intercalated and exfoliated (also called delaminated). In an intercalated structure one finds well-ordered multilayered structures in which the polymer chains are inserted between the galleries of the clay, thereby increasing the spacing between the galleries. On the other hand, in an exfoliated structure the individual silicate layers are spread such that they are no longer able to interact with the cations. Characterization of the formation of a nanocomposite, rather than the simple formation of an immiscible mixture of clay and polymer, requires the measurement of both the *d* spacing from X-ray diffraction, XRD, and transmission electron microscopy to determine the actual disposition of the clay within the polymer. In an immiscible mixture, the *d* spacing should be virtually identical to that of the starting clay, while if a nanocomposite is formed, the *d* spacing must increase. The formation of an exfoliated structure usually results in the complete loss of registry between the clay layers and no peak can be observed by XRD. The most likely occurrence has been the formation of some mixture of exfoliated and intercalated structures and this requires TEM measurements to show this fact.

The XRD data for all of the nanocomposites described herein and the starting clays are collected in Table 2. The *d* spacing is significantly larger for all of the organically modified clays than for the sodium clay, as expected because the organic cations are larger. The fact that no spacing is observed for the nanocomposite from VB-16 suggests, but does not prove, the formation of an exfoliated structure. In the other two cases, there is an increase in *d* spacing that indicates that a nanocomposite, rather than a simple immiscible blend, has been formed.

TEM Measurements on the Nanocomposites. The TEM images of the various nanocomposites are shown in Figures 3−5. The figures show both a larger view, showing the dispersion of the clay within the polymer, and a higher magnification, permitting the observation of discrete clay layers. For the VB-16 nanocomposite, one can see that the clay layers are isolated and that a largely exfoliated structure has been produced. At the other extreme, the OH-16 material appears to be almost entirely intercalated while P-16 shows a mixture of both

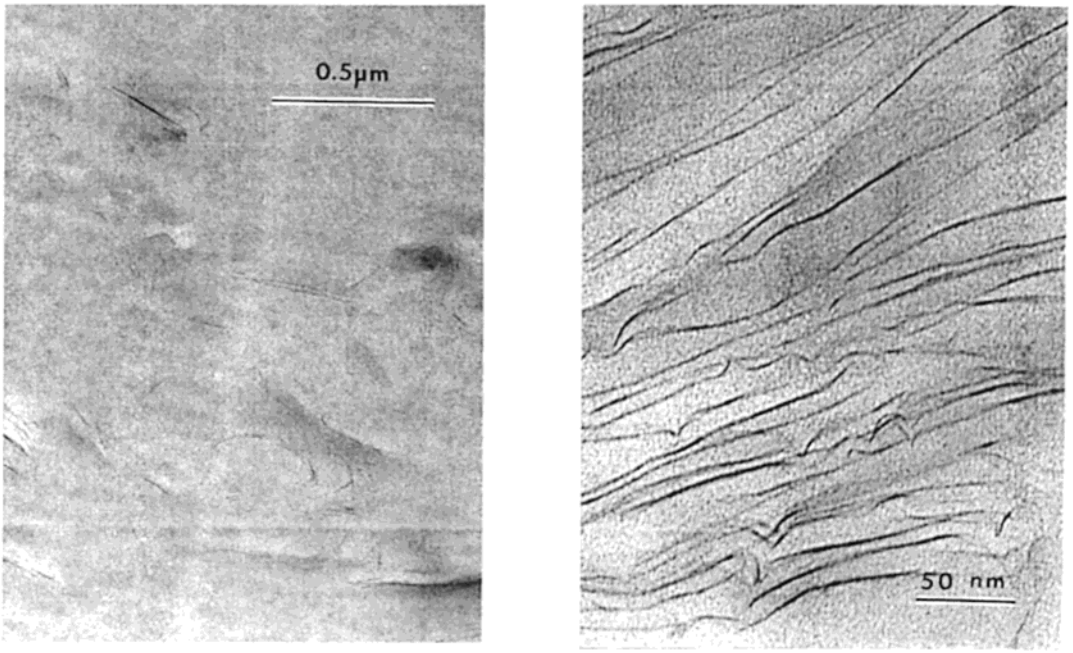

Figure 3. TEMs of the VB-16 nanocomposite at low (left) and higher (right) magnification.

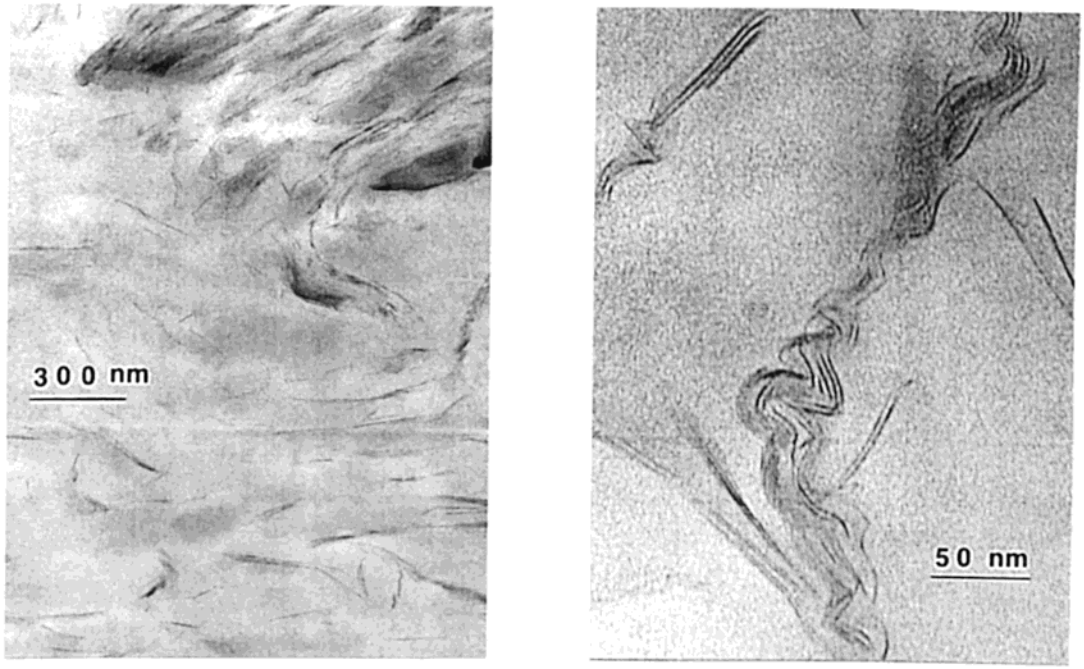

Figure 4. TEMs of the P-16 nanocomposites at low (left) and higher (right) magnifications.

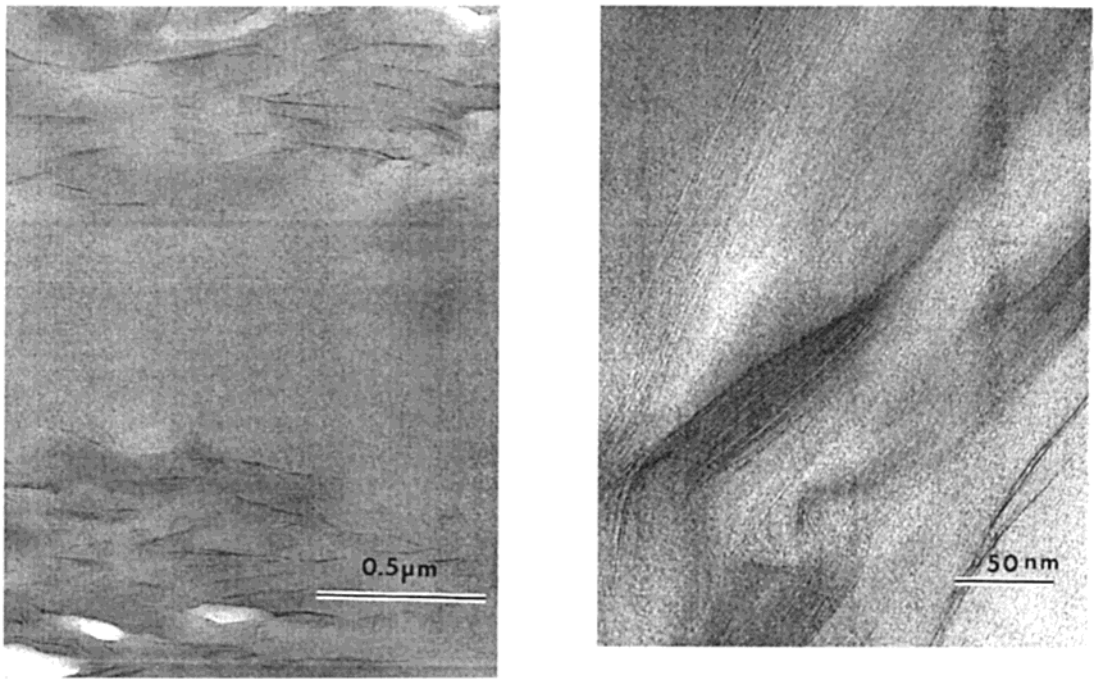

Figure 5. TEMs of the OH-16 nanocomposite at low (left) and higher (right) magnifications.

intercalated and exfoliated structures. Fu and Qutubuddin[9] have reported a polystyrene−clay nanocomposite in which the organic modification is essentially the same as that of the VB-16 reported in this work and they have also observed complete exfoliation for this material.

Mechanical Properties of the Nanocomposites. It is well-known that the mechanical properties of nanocomposites are enhanced relative to those of the polymer.[1] In this work, the strength at break and elongation at break have been measured for all three nanocomposites as representative of the mechanical properties. The strength at break increases by 300% for the VB-16 nanocomposite containing 3% clay; the increase is lower for the other nanocomposites, 120% for OH-16, and 90% for P-16. The elongation at break increases by 45% for VB-16 and is unchanged for OH-16 and P-16. The literature reports[1] that exfoliated nanocomposites have much higher mechanical properties than do intercalated systems and these data are confirmation of the TEM assignment.

TGA Characterization of Thermal Stability of the Nanocomposites. The thermal stability of the nanocomposite is enhanced relative to that of virgin polystyrene and this is shown in Figure 6. Typically, the onset temperature of the degradation is about 50 °C higher for the nanocomposites than for virgin polystyrene. If one looks very closely at the TGA curve for

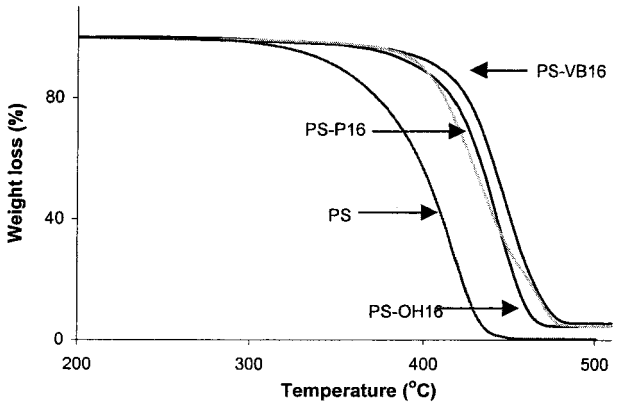

Figure 6. TGA curves for polystyrene, PS, and the nanocomposites.

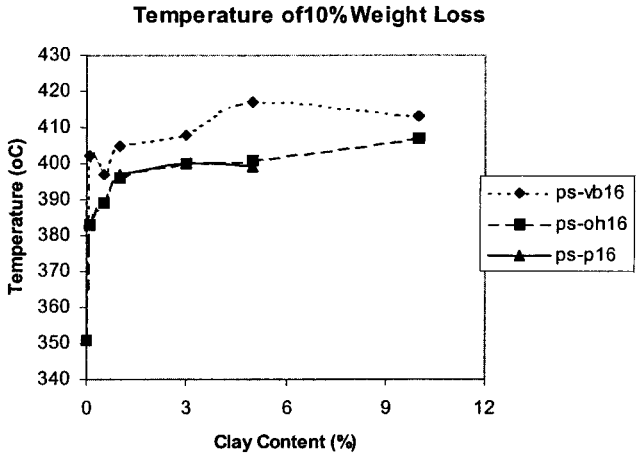

Figure 7. Temperature of 10% mass loss for nanocomposites as a function of the fraction of clay.

the phosphonium nanocomposite, one can see that there is a second step in the degradation, which is absent in the other two materials. This second step accounts for about 30% of the degradation of the phosphonium−polystyrene nanocomposite and must be attributed to some interaction between the clay and the polymer that serves to stabilize the nanocomposite. The most likely explanation is that the higher decomposition temperature of the phosphonium clay provides the formation of char at a more opportune time to retain the polymer. In the case of the ammonium clays char formation occurs earlier and can be broken up by the time that the polymer degrades.

The variation of the temperature at which 10% degradation occurs for all three nanocomposites is shown as a function of the amount of clay in Figure 7. Even with as little as 0.1% clay present in the nanocomposite, the onset temperature is significantly increased.

Fire Performance of Nanocomposites. One invariably finds that nanocomposites have a much lower peak heat release rate (PHRR) than does the virgin polymer; these materials follow this trend and all of the data are shown in Table 3; the peak heat release rate for polystyrene and the three nanocomposites is also shown graphically in Figure 8. All systems have been studied as a function of the amount of clay present and this is shown in Table 3 by a number following the legend of the sample, that is, P16-3 means that the nanocomposite was formed using 3% of P16 clay with

Table 3. Cone Calorimetry for the Polystyrene−Clay Nanocomposites

Polystyrene−VB-16 Nanocomposites				
composition	PS	PS−VB-16-1	PS−VB-16-3	PS−VB-16-5
time to ignition, s	35	20	45	35
PHRR, kW/m^2	1024	752	584	534
time to PHRR, s	165	165	185	180
time to burn out, s	190	212	226	230
energy released through 190 s	981	773	731	562
average HRR, kW/m^2	479	421	405	389
total heat released, kJ	1149	869	845	806
mass loss rate, mg/s	127	117	106	97
mass loss at 190 s, %	86	94	58	60
specific extinction area to 190 s, m/kg	1572	1070	1270	1052
Polystyrene−OH-16 Nanocomposites				
composition	PS	PS−OH16-1	PS−OH16-3	PS−OH16-5
time to ignition, s	35	15	23	
PHRR, kW/m^2	1024	766	502	429
time to PHRR, s	165	163	208	193
time to burn out, s	190	216	227	238
energy released through 190 s	981	845	658	493
average HRR, kW/m^2	479	462	396	341
total heat released, kJ	1149	1051	868	769
average mass loss rate, mg/s	127	140	114	96
mass loss at 190 s, %	86	84	70	54
specific extinction area to 190 s, m/kg	1572	892	922	957
Polystyrene−P-16 Nanocomposites				
composition	PS	PS−P-16-1	PS−P-16-3	PS−P-16-5
time to ignition, s	35	40	30	30
PHRR, kW/m^2	1024	749	586	496
time to PHRR, s	165	160	170	185
time to burn out, s	190	212	225	234
energy released through 190 s	981	702	597	525
average HRR, kW/m^2	479	459	392	348
total heat released, kJ	1149	918	824	730
mass loss rate, mg/s	127	121	107	93
mass loss at 190 s, %	86	76	66	58
specific extinction area to 190 s, m/kg	1572	1280	1416	1474

polystyrene. The peak heat release rate falls as the amount of clay increases. The suggested mechanism by which clay nanocomposites function involves the formation of a char that serves as a barrier to both mass and energy transport.[15] It is reasonable that as the fraction of clay increases, the amount of char that can be formed increases and the rate at which heat is released is decreased. There has been a suggestion that an intercalated material is more effective than is an exfoliated material in fire retardancy.[3] One of these nanocomposites, OH-16, is mostly intercalated and this gives a slightly larger reduction in the rate of heat release than do the other two systems, which contain a significant exfoliated fraction.

Concomitant with the decrease in the rate of heat release is a decrease in mass loss rate and the amount

(15) Gilman, J. W.; Jackson, C. L.; Morgan, A. B.; Harris, R., Jr.; Manias, E.; Giannelis, E. P.; Wuthenow, M.; Hilton, D.; Phillips, S. H. *Chem. Mater.* **2000**, *12*, 1866−1873.

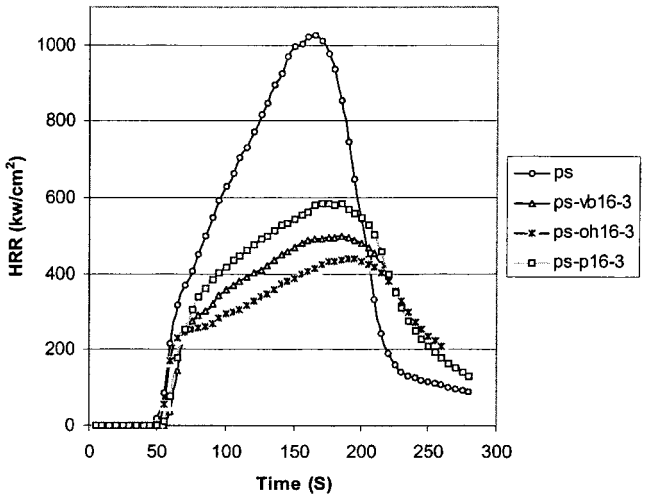

Figure 8. Peak heat release rates for polystyrene and the three nanocomposites.

of energy released by the time at which polystyrene has been entirely burned out and a modest increase in the time at which the peak heat release is reached. The production of a char barrier must serve to retain some of the polymer and thus both the energy released and the mass loss rate decrease. The amount of smoke evolved, specific extinction area, also decreases with the formation of the nanocomposite. There is some variability in the smoke production but apparently the formation of the nanocomposite gives a reduction in smoke, however, the presence of additional clay does not continue to decrease smoke.

Conclusions

Polystyrene−clay nanocomposites have been prepared that have structures that are intercalated, exfoliated, and a mixture of both forms. The exfoliated structure results when it is possible to initiate polymerization at the ammonium salt in the gallery of the clay. Thermogravimetric analysis has been used to characterize the degradation pathway of the clay organic treatment. Phosphonium clays have greater thermal stability than the corresponding ammonium salts and this may be useful when the polymer−clay mixture must be processed at relatively high temperatures. Thermogravimetric analysis of the nanocomposites shows that the onset of thermal degradation occurs at a higher temperature for the nanocomposites than for the virgin polymer. From cone calorimetry it is found that the rate of heat release is significantly reduced by the formation of the nanocomposites.

Acknowledgment. This work was performed under the sponsorship of the U.S. Department of Commerce, National Institute of Standards and Technology, Grant 60NANB6D0119. The assistance of Marcel van den Berk and David Paul, Solutia, Inc., in obtaining the cone calorimetric data is gratefully acknowledged. Also, certain commercial equipment, instruments, materials, or companies are identified in this paper to adequately specify the experimental procedure. This in no way implies endorsement or recommendation by NIST.

CM000984R